

# Restriction of Access to Dark State: A New Mechanistic Model for Heteroatom-Containing AIE Systems

Yujie Tu<sup>†,∇</sup>, Junkai Liu<sup>†,∇</sup>, Haoke Zhang<sup>†</sup>, Qian Peng<sup>§</sup>, Jacky W. Y. Lam<sup>†</sup>, Ben Zhong Tang<sup>\*†</sup>.

<sup>†</sup> Department of Chemistry, Hong Kong Branch of Chinese National Engineering Research Center for Tissue Restoration and Reconstruction and Institute for Advanced Study, The Hong Kong University of Science and Technology, Clear Water Bay, Kowloon, Hong Kong, China;

<sup>§</sup> Key Laboratory of Organic Solids, Beijing National Laboratory for Molecular Sciences, Institute of Chemistry, Chinese Academy of Sciences, Beijing 100190, China.

## Supporting Information Placeholder

**ABSTRACT:** Aggregation-induced emission (AIE) is an unusual photophysical phenomenon and provides an effective and advantageous strategy for the design of highly emissive materials in versatile applications such as sensing, imaging, and theragnosis. “restriction of intramolecular motion” is the well-recognized working mechanism of AIE and have guided the molecular design of most AIE materials. However, it sometimes fails to be workable to some heteroatom-containing systems. Herein, in this work, we take more than one excited state into account and specify a mechanism – “restriction of access to dark state (RADS)” – to explain the AIE effect of heteroatom-containing molecules. An anthracene-based zinc ion probe named APA is chosen as the model compound, whose weak fluorescence in solution is ascribed to the easy access from the bright ( $\pi,\pi^*$ ) state to the close-lying dark ( $n,\pi^*$ ) state caused by the strong vibronic coupling of the two excited states. By either metal complexation or aggregation, the dark state is less accessible due to the restriction of the molecular motion leading to the dark state and elevation of the dark state energy, thus the emission of the bright state is restored. RADS is found to be powerful in elucidating the photophysics of AIE materials with excited states which favor non-radiative decay, including overlap-forbidden states such as ( $n,\pi^*$ ) and CT states, spin-forbidden triplet states, which commonly exist in heteroatom-containing molecules.

Modern science usually obeys the reductionism basis to segment the complex entirety into elementary constituents. In reality, nature is so complicated that individual components cannot represent the feature of collective assemblies.<sup>1</sup> As science advances, some complementary disciplines have emerged to overcome the limitation of reductionism such as condensed matter physics<sup>2</sup> and systems biology<sup>3</sup>. The traditional researches in luminogenic material chemistry usually concern the property of isolated molecules in dilute solution as an ideal condition. However, the emission of many conventional dyes turns out to be quenched from solution to the solid state due to the aggregation-caused quenching (ACQ) effect.<sup>4</sup> Thus, photophysical behaviors of aggregates are often ignored until the discovery of “aggregation-induced emission

(AIE)” phenomenon in 2001,<sup>5</sup> which triggers the photophysical study in the aggregate/solid state.

Luminogens with AIE characteristics (AIEgens) often show weak or no emission in the isolated state but become highly emissive in an environment with constraints. AIE researches not only lead us to gain deeper insights into aggregate/solid state photophysics, but also provide a simple approach to modulate luminescence by controlling the state of aggregation, which is quite useful in analytical and biological applications such as sensing and imaging.<sup>6</sup> To aid the design of new AIEgens, elucidating the working mechanism of AIE is a prerequisite. Restriction of intramolecular motion (RIM) serves as a widely-accepted mechanism and clarifies the critical role of molecular motions in the light emission process.<sup>7</sup> Much work has been done to specify the exact motions and decay pathways,<sup>8</sup> making the connotation of RIM more accurate and detailed. So far, it is the most effective guideline for AIEgen design. It works well for pure hydrocarbon AIEgens. However, the AIE behaviors of heteroatom-containing AIEgens become complicated and sometimes cannot be fully explained by RIM. For example, a molecule can change its photophysical behaviors from AIE to ACQ by only altering one heteroatom.<sup>9</sup> Since heteroatoms are indispensable to achieve versatile functions and high biocompatibility, close investigation on the mechanism of heteroatom-containing AIEgens is of great significance.

Heteroatoms can generate rather complicated excited states. Firstly, heteroatoms often introduce the electron donating or withdrawing effect and help the formation of a weakly emissive charge transfer (CT) state with orbital spatial separation.<sup>10</sup> Secondly, heteroatoms import non-bonding orbitals originated from their lone-pair electrons to give rise to ( $n,\pi^*$ ) transitions. Similar to CT state, ( $n,\pi^*$ ) state is an overlap-forbidden state with a very small molar absorptivity ( $\epsilon$ ) and nearly zero oscillator strength ( $f$ ).<sup>11</sup> Thirdly, according to the El Sayed’s rule,<sup>12</sup> ( $n,\pi^*$ ) state will facilitate the intersystem crossing to triplet states which are spin-forbidden, long-lived and can be quenched easily. Herein, we define an excited state which obeys forbiddingness (supporting information) and is detrimental to luminescence as a “dark state”. It is a descriptive concept relative to the luminescent ( $\pi,\pi^*$ ) “bright state”. These emerging dark states contribute to a deeper understanding of the emission behaviors of AIEgens.

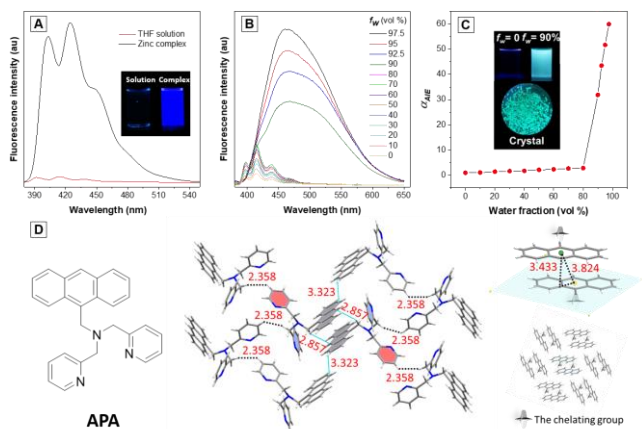


**Figure 1.** (A) PL spectra of free APA molecule and its complex with zinc ion in THF solution, (B) PL spectra of APA in THF/water mixtures with different water fractions ( $f_w$ ). (C) The plot of  $\alpha_{AIE}$  ( $I/I_0$ ) versus  $f_w$  at 461 nm,  $[APA] = 10^{-4}$  M,  $\lambda_{ex} = 350$  nm, where  $I_0$  is the PL intensity in pure THF. (D) Molecular structure and crystal packing structures of APA. Blue dash: C-H  $\cdots$   $\pi$  interaction. Black dashes: distances.

In this work, we take a unique AIE-active molecule called (9-anthrylmethyl)bis(2-pyridylmethyl)amine (APA) with a well-known nitrogen-containing zinc ion chelating unit and a pure hydrocarbon reporting unit as a model compound for the present study (Fig. 1D). As a sensitive zinc ion probe,<sup>13</sup> APA was applied in environmental analysis and zinc ion quantification in our previous study.<sup>14</sup> Its quenching effect was empirically ascribed to photo-induced electron transfer (PET).<sup>15</sup> However, the real photophysical process remains a black box, and the present explanation faces challenges and should be amended from quantum-chemical views (Supporting information).<sup>16</sup> APA shows unique AIE property, which is unexpected as commonly reported AIEgens generally possess multiple conjugated rotors.<sup>6</sup> Although a few anthracene-based AIEgens are explored, they are conjugated to a certain extent.<sup>17, 8e</sup> Therefore, it is anticipated to obtain potential implications in AIE mechanism via studying the varied photophysical processes of APA in different experimental conditions.

APA shows weak emission in dilute THF solution with a quantum yield ( $\Phi_f$ ) of 0.6 %. Its spectrum exhibits well-defined vibronic peaks of anthracene derivatives. After chelation with zinc ion, the resulting complex emits intensely with a  $\Phi_f$  of  $\sim 100\%$  and similar vibronic peaks (Fig. 1A). On the other hand, when

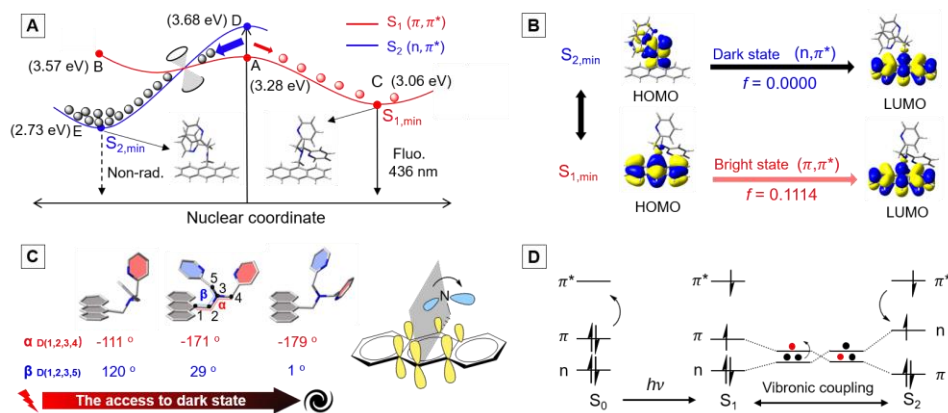


**Figure 2.** (A) Schematic potential energy surfaces of two close-lying excited states of APA in the gas phase. (B) Molecular orbitals for the corresponding electronic transitions at the  $S_{1,min}$  and  $S_{2,min}$ . (C) Demonstration of molecular motion by 3 selected representative geometries along the pathway from bright conformation to  $S_{2,min}$ , dihedral angles D(1,2,3,4) and D(1,2,3,5) are chosen as the dominant structural parameters. (D) FMO energy diagrams of deactivation mechanism.

**Table 1. The photophysical parameters of APA<sup>a</sup>**

	$\lambda_{em}$ (nm)	$\Phi_f$ (%)	$k_r$ ( $\times 10^6$ s <sup>-1</sup> )	$k_{nr}$ ( $\times 10^6$ s <sup>-1</sup> )
Solution	392,413,438	0.6	6.39	1060
Aggregate <sup>c</sup>	461	2.8	9.09	316
Crystal	492	39	10.3	16.1
Complex	403,424,447	99.8	101	0.202

<sup>a</sup>Abbreviation:  $\lambda_{em}$  = emission maximum,  $\Phi_f$  = fluorescence quantum yield,  $k_r$  = radiative decay rate constant =  $\Phi_f/\tau_f$ ,  $k_{nr}$  = non-radiative decay rate constant =  $(1 - \Phi_f)/\tau_f$ , where  $\tau_f$  = fluorescence lifetime. <sup>b</sup>In THF/H<sub>2</sub>O mixture with 90% water fraction.

more than 90% water was added to the THF solution of APA, a distinct broad, structureless, and red-shifted emission band with enhanced emission intensity was detected at 461 nm due to the aggregate formation. The large spectral discrepancy between the complex and aggregate peaks indicates that the emission originates from different excited states or different emitting species. The APA crystals display a similar emission band at 492 nm (Fig. S1, in the supporting information) and an antiparallel dimeric packing pattern, indicating the aggregate emission stems from dimers. As shown in figure 1D, the dimers are rigidified tightly with multiple effective C-H  $\cdots$   $\pi$  interactions, and the chelating units are stuck in a twisted conformation and packed closely to the neighbors (2.358 Å). Two face-to-face anthracene moieties with obvious intermolecular  $\pi$ - $\pi$  interactions are observed with an interplanar distance of 3.433 Å. Due to the sandwich herringbone packing pattern, every dimer is separated from other pairs.

To further understand the emission process, the rates of radiative ( $k_r$ ) and non-radiative ( $k_{nr}$ ) decay were calculated based on the quantum yields and lifetimes (Table. 1 and S1, Fig. S1). from solution to aggregate suspension and then crystal, the degree of molecular freedom gradually decreases, the  $k_{nr}$  values dramatically decline while the  $k_r$  values increase slightly. These results are in accord with commonly-reported results of RIM.<sup>18</sup> Surprisingly, when the nitrogen atoms of APA complex with zinc ion, the resulting complex shows not only a drastically suppressed  $k_{nr}$  by 4-order of magnitude but also a greatly enhanced  $k_r$ . A hypothesis can be naturally raised that both RIM and lone pairs participate in the light emission processes.

To prove this, more than one excited state was considered including transitions of non-bonding orbitals. We optimized the

structures of isolated APA in the ground state and the first two excited states. At the Frank-Condon region, two close-lying excited states are assigned as  $S_1$  state of  $(\pi, \pi^*)$  character and  $S_2$  state of  $(n, \pi^*)$  character (Fig. 2B). The schematic illustration of the potential energy surfaces (PES) of the two excited states was plotted (Fig. 2A). After vertical excitation, the excitons are supposed to undergo two competing pathways: 1) relaxation on the  $S_1$  PES to reach the bright  $(\pi, \pi^*)$   $S_{1,\min}$  ( $f = 0.1114$ ), resulting in fluorescence at 436 nm which is consistent with the experimental data, 2) internal conversion to a dark  $(n, \pi^*)$   $S_{2,\min}$  ( $f = 0.0000$ ) via the conical intersection of  $S_1$  and  $S_2$ , leading to fast non-radiative decay. Since the  $S_{2,\min}$  is lower in energy than  $S_{1,\min}$ , the second pathway dominates with overwhelming exciton population to result in weak fluorescence and short lifetime. The relaxation to the dark state minimum is governed by a certain pattern of molecular motions along the PES, which vibronically couples the two excited states. To visualize the molecular motion and the access to the dark state, several intermediate geometries along the relaxation pathway to  $S_{2,\min}$  were extracted (Fig. 2C). The two dihedral angles  $\alpha$  and  $\beta$  both change from around  $120^\circ$  (trigonal pyramidal) to  $0^\circ$  (planar). In other words, relative to the  $\pi$  orbitals of the anthracene plane, the direction of lone pair on the alkyl nitrogen changes from an orientation beneficial for  $n$ - $\pi$  orbital overlap to an orthogonal orientation (Fig. 2C). From the perspective of frontier molecular orbitals, as the “fan rotation” goes, the molecular geometry approaches the  $S_1/S_2$  conical intersection where an electron transfer from  $n$  to  $\pi$  orbital occurs accompanied with the inversion of the close-lying  $n$  and  $\pi$  orbitals. Consequently, the HOMO changes from  $\pi$  to  $n$  orbital, then the LUMO-to-HOMO transition becomes a dark  $(n, \pi^*)$  transition to quench the emission.

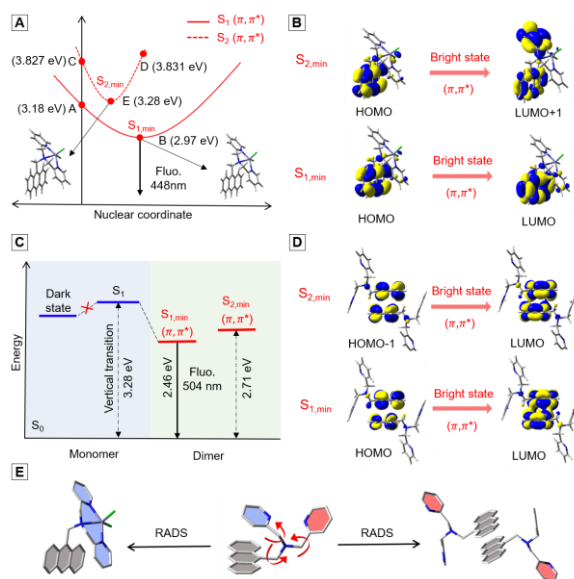


**Figure 3.** (A) Schematic PESs of  $S_1$  and  $S_2$  of zinc complex in the gas phase. (C) Energy levels of APA monomer and dimer. Molecular orbitals for the electronic transitions at the  $S_{1,\min}$  and  $S_{2,\min}$  of (B) complex and (D) crystal. (E) Schematic illustration of RIM induced RADS due to complexation and dimer formation.

Now we understand that the quenching process is a molecular motion and electron transfer-mediated dark state population. Herein, it is anticipated that the fluorescence will be restored if the access to dark state is restricted by either freezing the corresponding molecular motions or blocking the  $n \rightarrow \pi$  electron transfer. By examining the excited states of the complex and crystal, the hypothesis was verified. For the complex, the lone pair elec-

trons of the three nitrogen atoms are occupied by zinc ion coordination, and the non-bonding orbitals participate in bond formation. Thereupon the  $(n, \pi^*)$  transition is elevated to higher energy levels. Both the  $S_1$  and  $S_2$  are now  $(\pi, \pi^*)$  transitions without any crossing on the PES (Fig. 3A and 3B, Table S2 and S3). Meanwhile, the chelating unit is highly rigidified, and the resulting chelate exerts strong steric hindrance to the anthracene unit. The two bulky planar structures lock each other in a twisted conformation, so the non-radiative decay at the bright state can be further suppressed. Both effects collectively lead to an ultimate  $\Phi_f$  of  $\sim 100\%$ . As for the crystal, the molecules are closely packed, and various intermolecular interactions rigidify them tightly. Therefore, the motions leading to the dark state conformation are restricted. Moreover, unlike the free monomer, the dimer as a whole unit has completely different electronic states due to the effective through-space conjugation between the anthracene moieties and the exciton splitting (Fig. 3C and 3D, Table S4 and S5). Such observation was often found in anthracene-based dimers.<sup>19</sup> As calculated, no  $(n, \pi^*)$  character from  $S_1$  to  $S_4$  can be identified (Table. S6 and S7), which means that the  $(n, \pi^*)$  deactivation pathway in the free molecules is no longer active in dimers. In a nutshell, by either coordination or crystallization, the molecular motion leading to the originally dominant dark state can be restricted, resulting in the decoupling of the bright and dark states. This is indicated by both the disappearance of low-lying  $(n, \pi^*)$  state and the nearly no nuclear displacement in the conformations of  $S_{0,\min}$ ,  $S_{1,\min}$ , and  $S_{2,\min}$  (Fig. 3B and 3D, Table S5 and S7).

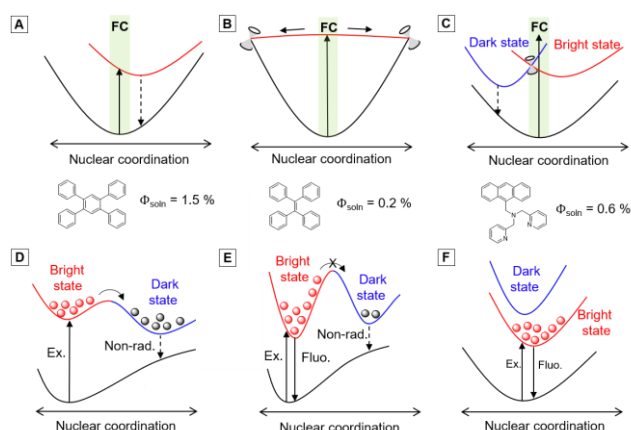


**Figure 4.** Schematic illustrations of nonradiative decay in the solution state via (A) strong  $S_1$ - $S_0$  vibronic coupling, (B) conical intersection, (C) internal conversion to the close-lying dark state. (D) fluorescence quenching by bright-dark state vibronic coupling. Restriction of access to dark state by (E) restriction of molecular motion and (F) increasing the energy of the dark state.

Above all, we have gained quantum-chemical insights into the dark state mediated non-radiative decay process and illustrated two light-up approaches based on the APA molecule. We can conclude a new mechanism, namely “restriction of access of dark state” (RADS) to complete the picture of AIE mechanism (Fig. 3E). The previous mechanistic research concerns only the vibronic coupling between  $S_1$  and  $S_0$  to explain the non-emissive nature of motor-rich molecules in solution (Fig. 4A). As an extreme scenario of vibronic coupling, deactivation via conical intersection was also gradually accepted (Fig. 4B).<sup>8b, 8c, 20</sup> However, few works considered higher excited states.<sup>21</sup> In fact, as presented in this work, multiple excited states are involved in governing the photophysical process of AIEgens. Especially for heteroatom-containing systems, the PESs of different excited states arrange in

a complicated manner, and the presence of accessible dark state (CT, ( $n,\pi^*$ ), triplet state, etc.) that crosses the luminescent ( $\pi,\pi^*$ ) state on the PES will lead to fast non-radiative transitions. Therefore, a three-state model should be considered (Fig. 4C and 4D). Once the nuclear motions approaching the dark state encounter constraints (Fig. 4E) or the energy of the dark state is pushed upwards under certain conditions such as aggregation (Fig. 4F), the emission will be restored because of the RADS mechanism.

## ASSOCIATED CONTENT

### Supporting Information

The supporting material is available free of charge via the Internet at <http://pubs.acs.org>. Background information, detailed methods, supplementary experimental and computational results (PDF). The Supporting Information is available free of charge on the ACS Publications website.

## AUTHOR INFORMATION

### Corresponding Author

\*tangbenz@ust.hk

### Author Contributions

<sup>†</sup>Y.T. and J.L. contributed equally.

### Notes

The authors declare no competing financial interest.

## ACKNOWLEDGMENT

We are grateful for financial support from the National Science Foundation of China (21788102 and 81501591), the Research Grants of Council of Hong Kong (16308016, A-HKUST605/16, and C6009-17G), the Innovation of Technology Commission (ITC-CNERC14SC01), and the Science and Technology Plan of Shenzhen (JCY20160229205601482).

## REFERENCES

- (1) Gallagher, R.; Appenzeller, T. Beyond reductionism - Introduction. *Science*. **1999**, *284*, 79-79.
- (2) Pietronero, L. Complexity ideas from condensed matter and statistical physics. *Europhysics News*. **2008**, *39*, 26-29.
- (3) Ahn, A. C.; Tewari, M.; Poon, C. S.; Phillips, R. S. The limits of reductionism in medicine: could systems biology offer an alternative? *PLoS Med*. **2006**, *3*, e208.
- (4) Birks, J. B. Photophysics of aromatic molecules. **1970**.
- (5) Luo, J.; Xie, Z.; Lam, J. W. Y.; Cheng, L.; Tang, B. Z.; Chen, H.; Qiu, C.; Kwok, H. S.; Zhan, X.; Liu, Y.; Zhu, D. Aggregation-induced emission of 1-methyl-1,2,3,4,5-pentaphenylsilole. *Chem. Commun.* **2001**, 1740-1741.
- (6) Mei, J.; Leung, N. L. C.; Kwok, R. T. K.; Lam, J. W. Y.; Tang, B. Z. Aggregation-Induced Emission: Together We Shine, United We Soar! *Chem. Rev.* **2015**, *115*, 11718-11940.
- (7) Leung, N. L.; Xie, N.; Yuan, W.; Liu, Y.; Wu, Q.; Peng, Q.; Miao, Q.; Lam, J. W.; Tang, B. Z. Restriction of intramolecular motions: the general mechanism behind aggregation-induced emission. *Chemistry (Easton)*. **2014**, *20*, 15349-53.
- (8) (a) Tseng, N.-W.; Liu, J.; Ng, J. C. Y.; Lam, J. W. Y.; Sung, H. H. Y.; Williams, I. D.; Tang, B. Z. Deciphering mechanism of aggregation-induced emission (AIE): Is E-Z isomerisation involved in an AIE process? *Chem. Sci.* **2012**, *3*, 493-497; (b) Li, Q.; Blancafort, L. A conical intersection model to explain aggregation induced emission in diphenyl dibenzofulvene. *Chem. Commun.* **2013**, *49*, 5966-8; (c) Peng, X.-L.; Ruiz-Barragan, S.; Li, Z.-S.; Li, Q.-S.; Blancafort, L. Restricted access to a conical intersection to explain aggregation induced emission in dimethyl tetraphenylsilole. *J. Mater. Chem. C*. **2016**, *4*, 2802-2810; (d) Prlj, A.;

- Doslic, N.; Corminboeuf, C. How does tetraphenylethylene relax from its excited states? *Phys. Chem. Chem. Phys.* **2016**, *18*, 11606-9; (e) Sasaki, S.; Suzuki, S.; Sameera, W. M.; Igawa, K.; Morokuma, K.; Konishi, G. Highly Twisted N,N-Dialkylamines as a Design Strategy to Tune Simple Aromatic Hydrocarbons as Steric Environment-Sensitive Fluorophores. *J. Am. Chem. Soc.* **2016**, *138*, 8194-206; (f) Gao, Y. J.; Chang, X. P.; Liu, X. Y.; Li, Q. S.; Cui, G.; Thiel, W. Excited-State Decay Paths in Tetraphenylethene Derivatives. *J. Phys. Chem. A*. **2017**, *121*, 2572-2579; (g) Cai, Y.; Du, L.; Samedov, K.; Gu, X.; Qi, F.; Sung, H. H. Y.; Patrick, B. O.; Yan, Z.; Jiang, X.; Zhang, H.; Lam, J. W. Y.; Williams, I. D.; Lee Phillips, D.; Qin, A.; Tang, B. Z. Deciphering the working mechanism of aggregation-induced emission of tetraphenylethylene derivatives by ultrafast spectroscopy. *Chem. Sci.* **2018**, *9*, 4662-4670; (h) Xiong, J. B.; Yuan, Y. X.; Wang, L.; Sun, J. P.; Qiao, W. G.; Zhang, H. C.; Duan, M.; Han, H.; Zhang, S.; Zheng, Y. S. Evidence for Aggregation-Induced Emission from Free Rotation Restriction of Double Bond at Excited State. *Org. Lett.* **2018**, *20*, 373-376; (i) Crespo-Otero, R.; Li, Q.; Blancafort, L. Exploring Potential Energy Surfaces for Aggregation-Induced Emission-From Solution to Crystal. *Chem. Asian J.* **2019**, *14*, 700-714; (j) Zhang, H.; Liu, J.; Du, L.; Ma, C.; Leung, N. L. C.; Niu, Y.; Qin, A.; Sun, J.; Peng, Q.; Sung, H. H. Y.; Williams, I. D.; Kwok, R. T. K.; Lam, J. W. Y.; Wong, K. S.; Phillips, D. L.; Tang, B. Z. Drawing a clear mechanistic picture for the aggregation-induced emission process. *Mater. Chem. Front.* **2019**.
- (9) (a) Yoshii, R.; Nagai, A.; Tanaka, K.; Chujo, Y. Highly emissive boron ketoiminate derivatives as a new class of aggregation-induced emission fluorophores. *Chemistry (Easton)*. **2013**, *19*, 4506-12; (b) Nie, H.; Hu, K.; Cai, Y.; Peng, Q.; Zhao, Z.; Hu, R.; Chen, J.; Su, S.-J.; Qin, A.; Tang, B. Z. Tetraphenylfuran: aggregation-induced emission or aggregation-caused quenching? *Mater. Chem. Front.* **2017**, *1*, 1125-1129.
- (10) (a) Grabowski, Z. R.; Rotkiewicz, K.; Rettig, W. Structural changes accompanying intramolecular electron transfer: Focus on twisted intramolecular charge-transfer states and structures. *Chem. Rev.* **2003**, *103*, 3899-4031; (b) Liese, D.; Haberhauer, G. Rotations in Excited ICT States - Fluorescence and its Microenvironmental Sensitivity. *Isr. J. Chem.* **2018**, *58*, 813-826.
- (11) Turro, N. J., *Modern molecular photochemistry*. University science books: 1991.
- (12) Lower, S.; El-Sayed, M. The triplet state and molecular electronic processes in organic molecules. *Chem. Rev.* **1966**, *66*, 199-241.
- (13) Zhang, L.; Clark, R. J.; Zhu, L. A heteroditopic fluoroionophoric platform for constructing fluorescent probes with large dynamic ranges for zinc ions. *Chemistry (Easton)*. **2008**, *14*, 2894-903.
- (14) Leung, C.; Tu, Y.; Tang, B. Z.; Wang, W.-X. Dissolution Kinetics of Zinc Oxide Nanoparticles: Real-time Monitoring by a Zn<sup>2+</sup>-specific Fluorescent Probe. *Environ. Sci. Nano*. **2019**.
- (15) Kubo, K.; Mori, A. PET fluoroionophores for Zn<sup>2+</sup> and Cu<sup>2+</sup>: complexation and fluorescence behavior of anthracene derivatives having diethylamine, N-methylpiperazine and N,N-bis(2-picoly)amine units. *J. Mater. Chem.* **2005**, *15*, 2902.
- (16) Escudero, D. Revising Intramolecular Photoinduced Electron Transfer (PET) from First-Principles. *Acc. Chem. Res.* **2016**, *49*, 1816-24.
- (17) Sasaki, S.; Igawa, K.; Konishi, G.-i. The effect of regioisomerism on the solid-state fluorescence of bis(piperidyl)anthracenes: structurally simple but bright AIE luminogens. *J. Mater. Chem. C*. **2015**, *3*, 5940-5950.
- (18) (a) Peng, Q.; Yi, Y.; Shuai, Z.; Shao, J. Toward quantitative prediction of molecular fluorescence quantum efficiency: Role of Duschinsky rotation. *J. Am. Chem. Soc.* **2007**, *129*, 9333-9339; (b) Zhang, T.; Jiang, Y.; Niu, Y.; Wang, D.; Peng, Q.; Shuai, Z. Aggregation effects on the optical emission of 1,1,2,3,4,5-hexaphenylsilole (HPS): a QM/MM study. *J. Phys. Chem. A*. **2014**, *118*, 9094-104.
- (19) (a) Kaanumalle, L. S.; Gibb, C. L. D.; Gibb, B. C.; Ramamurthy, V. A hydrophobic nanocapsule controls the photophysics of aromatic molecules by suppressing their favored solution pathways. *J. Am. Chem. Soc.* **2005**, *127*, 3674-3675; (b) Liu, H.; Yao, L.; Li, B.; Chen, X.; Gao, Y.; Zhang, S.; Li, W.; Lu, P.; Yang, B.; Ma, Y. Excimer-induced high-efficiency fluorescence due to pairwise anthracene stacking in a crystal with long lifetime. *Chem. Commun.* **2016**, *52*, 7356-9.
- (20) Tran, H.; Prlj, A.; Lin, K. H.; Hollas, D.; Corminboeuf, C. Mechanisms of fluorescence quenching in prototypical aggregation-induced emission systems: excited state dynamics with TD-DFTB. *Phys. Chem. Chem. Phys.* **2019**.
- (21) Qian, H.; Cousins, M. E.; Horak, E. H.; Wakefield, A.; Liptak, M. D.; Aprahamian, I. Suppression of Kasha's rule as a mechanism for fluorescent molecular rotors and aggregation-induced emission. *Nat. Chem.* **2017**, *9*, 83-87.

